act as an electron scavenger.

In conclusion, the ESR spectra from poly(chloroprene) uniaxially deformed at 77 K in an oxygen environment are composite spectra arising from two radical species. An allyl radical species results from main-chain rupture midway between the α-methylene groups, and a peroxy radical species is formed by reaction of the oxygen in the environment with the allyl radical species. The stability of these allyl radicals with respect to oxygen and temperature is apparently similar to the allyl radicals formed in polybutadiene and polyisopropene. At liquid nitrogen temperature all the radicals were stable. The peroxy radical species is unstable as T_g is approached and decays to give a resonance-stabilized allylic species, which is stable until the temperature of the sample is slightly above T_g. Above T_g a broad singlet is observed and is attributed to a polyenyl radical species.

References and Notes

(1) V. T. Kozlov and Z. N. Tarasova, *Vysokomol. Soedin.*, 8, 943 (1966).
(2) P. Carstensen, Nobel Symposium 22, "Degradation of 1,4-Polydienes Induced by Ultraviolet Irradiation", Per-Olof Kinell, B. Rånby, and V. Runnstrom Reio, Eds., p 159.
(3) P. Carstensen, *Acta Polytech. Scand., Chem. Incl. Metall. Ser.*, **No. 97** (1970).
(4) P. Carstensen, *Makromol. Chem.*, **135**, 219 (1970).
(5) P. Carstensen, *Makromol. Chem.*, **142**, 131, 145 (1971).
(6) B. Reeve, Ph.D. Thesis, University of London, 1972, Chapter 6.
(7) E. H. Andrews and P. E. Reed, "Deformation and Fracture of High Polymers", H. H. Kausch, J. A. Hassell, and R. I. Jaffee, Eds., Plenum, New Yrok, 1973, p 259.
(8) A. Tager, "Physical Chemistry of Polymers", Mir. Publishing Co., Moscow (1970).
(9) W. T. Mead and P. E. Reed, *Polym. Eng. Sci.*, **14**, 22 (1974).
(10) W. T. Mead, R. S. Porter, and P. E. Reed, *Macromolecules*, **11**, 56 (1978).
(11) E. H. Andrews, *Pure Appl. Chem.*, **31**, 91 (1972).
(12) E. H. Andrews and B. Reeve, *J. Mater. Sci.*, **6**, 547 (1971).
(13) R. M. Murray and D. C. Thompson, "The Neoprenes", E. I. DuPont De Nemours and Co., 1963.
(14) K. U. Ingold and J. R. Morton, *J. Am. Chem. Soc.*, **86**, 3400 (1964).
(15) B. Rånby and J. F. Rabek, "Photodegradation, Photo-oxidation and Photostabilization of Polymers", Wiley, London, 1975, p 98.
(16) L. A. Blyumenfield, A. A. Berlin, A. A. Slinkin, and A. E. Kalmanson, *Strukt. Khim.*, 1, 103 (1960).
(17) M. Sakaguchi and J. Sohma, *Polym. J.*, **7**, 490 (1975).

Entanglement Networks of 1,2-Polybutadiene Cross-Linked in States of Strain. 8. Trapping of Entanglements in Relaxed and Unrelaxed Configurations

Hsin-Chia Kan and John D. Ferry*

Department of Chemistry, University of Wisconsin, Madison, Wisconsin 53706.

Received February 27, 1979

ABSTRACT: A sample of 1,2-polybutadiene (T_g = −10 °C) is strained in uniaxial extension to a stretch ratio λ_0 at 0 °C, allowed to relax at constant strain for time t_R, cooled to −10 °C, and cross-linked by γ irradiation, thereby trapping a proportion of the entanglements originally present. The network strands contributed by the trapped entanglements are partly in strained configurations (ν_N mol/cm^3) and partly in relaxed (randomized) configurations (ν_{NR} mol/cm^3). Upon release and warming, the sample seeks a state of ease with stretch ratio λ_s in which the forces associated with the trapped unrelaxed entanglements balance the forces associated with the trapped relaxed entanglements and the cross-links. The strand densities ν_N, ν_{NR}, and ν_X (density of network strands contributed by cross-links) can be calculated from measurements of λ_0, λ_s, and the equilibrium tensile stress at λ_0, for various values of t_R and various degrees of cross-linking by different irradiation doses. Based on a two-network model, the stress at any subsequent strain λ is accurately given by the sum $\sigma_N + \sigma_Y$, where σ_N is the stress contributed by a network of trapped unrelaxed entanglements with $\lambda = 1$ as a reference state and σ_Y is the stress contributed by a network of cross-links and trapped relaxed entanglements with $\lambda = \lambda_0$ as a reference state. With increasing t_R at constant dose, ν_X is constant, ν_N decreases, and ν_{NR} is zero until a critical value of t_R is reached and then increases. The trapping probabilities $T_{e,u}$ and $T_{e,r}$ for unrelaxed and relaxed entanglements, respectively, are estimated and compared with the Langley theory. At low values of t_R, $T_{e,u}$ agrees with the Langley theory and $T_{e,r}$ is zero. Beyond a critical value of t_R, $T_{e,u}$ increases and $T_{e,r}$ becomes finite and increases but remains lower than the average value predicted by the Langley theory. The behavior is consistent with the terminal mechanism of relaxation in the tube theory of Doi and Edwards in which the unrelaxed entanglements correspond to topological restraints near the center of the tube contour, and the relaxed entanglements correspond to constraints on the ends of the molecule which have found new tube paths by reptation.

The cross-linking of 1,2-polybutadiene strained in simple extension has been described in previous papers of this series.[1-5] When a strained sample with stretch ratio λ_0 is cross-linked with γ irradiation near the glass transition temperature (T_g), the resulting cross-link network traps the entanglements originally present; after release and warming, the sample seeks a state of ease with stretch ratio λ_s in which the forces associated with the cross-links and the trapped entanglements act in opposite directions. From λ_0 and λ_s, together with stress–strain measurements in extension from the state of ease, or simply from the equilibrium stress at λ_0, the concentration of trapped entanglement strands ν_N can be calculated on the basis of a dual network model and compared with the entanglement strand density estimated from transient measurements on the uncross-linked polymer. To obtain consistent results, especially for stress–strain relations in large extensions of the dual network from its state of ease, it is necessary to attribute deviations from neo-Hookean elasticity to the trapped entanglement network, as de-

0024-9297/79/2212-0494$01.00/0

Table I
Summary of Sample History in Experimental Procedure

	unstretched	stretched, held t_R, s	irradiated by ^{60}Co	stress released	stress relaxation	stress-strain measurements
stretch ratio, λ	1	λ_0 ($\simeq$ 1.6)	λ_0	λ_s	λ_0' ($\simeq \lambda_0$)	λ
temp, °C	0	0	−10	~23	⩾20	50
strand densities due to various types of entanglements	total: ν_e^0	unrelaxed: $\nu_e(t_R)$	trapped: $\nu_N = T_{e,u}\nu_e(t_R)$		partially unrelaxed during approach to equilibrium	
			untrapped		relaxed at equilibrium	
		relaxed: $\nu_e^0 - \nu_e(t_R)$	trapped: $\nu_{NR} = T_{e,r}[\nu_e^0 - \nu_e(t_R)]$		partially unrelaxed during approach to equilibrium	
			untrapped		relaxed at equilibrium	

scribed for example by the Mooney–Rivlin equation; whereas the cross-link network appears to be simply neo-Hookean. The proportion of entanglements trapped increases toward unity with increasing degree of cross-linking, in general agreement with the theory of Langley[6] for random cross-linking in the unstrained state.

In paper 3, it was noted[2] that if irradiation was performed a few degrees above T_g, the density of trapped entanglement strands ν_N calculated in the above manner was considerably smaller even at doses sufficiently high so that most of the entanglements should be trapped in Langley's sense. The difference was attributed to partial relaxation of strained configurations during cross-linking so that some entanglements were trapped corresponding to unstrained (randomized) configurational distributions. If relaxation occurs during the cross-linking process in this manner, the resulting network is very complicated and difficult to analyze. To study entrapment in relaxed and unrelaxed configurations, it is better to allow initial controlled relaxation at constant strain first and then irradiate at a temperature sufficiently low to prevent further relaxation. The present paper describes such experiments (see Table I), which permit estimation of the trapping probabilities for relaxed and unrelaxed entanglements separately.

Theory

It is assumed that, during stress relaxation at constant stretch ratio λ_0, the total density of entanglement strands ν_e^0 (mol/cm^3) remains constant; the density of unrelaxed strands is $\nu_e(t)$, a decreasing function of time t, and that of relaxed strands is $\nu_e^0 - \nu_e(t)$. (Neglect of any intermediate degrees of relaxation is plausible in the light of the tube theory of Doi and Edwards[7] for the relaxation process and has been used successfully to interpret recovery of partially relaxed uncross-linked entanglement networks.[8])

After initial relaxation for a period t_R, cross-linking traps both unrelaxed and relaxed entanglements to produce the following densities respectively:

$$\nu_N = T_{e,u}\nu_e(t_R) \quad (1)$$

$$\nu_{NR} = T_{e,r}[\nu_e^0 - \nu_e(t_R)] \quad (2)$$

where the T_e's are the trapping probabilities for unrelaxed and relaxed entanglements, respectively. In previous treatments, only ν_N and $T_{e,u}$ were considered. The relaxed entanglement strands, like those contributed (terminated) by cross-links (with density ν_X), are in their undeformed reference configurations at the macroscopic stretch ratio λ_0. In the state of ease following release of stress, the dual network model corresponds to a network of ν_N strands in extension and one of $\nu_X + \nu_{NR} \equiv \nu_Y$ strands in compression.

As before, the N network of (ν_N strands) is assigned the Mooney–Rivlin coefficients C_{1N} and C_{2N}; the Y network (of ν_Y strands) is taken as neo-Hookean with C_{1Y} only, since it is in compression, following the same reasoning as used previously for the ν_X network for conditions when ν_{NR} = 0. (Reservations concerning use of the Mooney–Rivlin formulation and its justification for convenience have been expressed elsewhere.[5,9]) Then, assuming front factors of unity, the *strand* densities are related to the Mooney–Rivlin coefficients as follows:

$$\nu_N = (2/RT)(C_{1N} + C_{2N}) \quad (3)$$

$$\nu_Y = (2/RT)C_{1Y} \quad (4)$$

The relative magnitudes of C_{1N} and C_{2N} are, as before, expressed by the ratio $\psi_N = C_{2N}/(C_{1N} + C_{2N})$, which depends on the degree of initial relaxation and has been determined experimentally as a function of relaxation period from nonlinear stress relaxation measurements on the uncross-linked polymer used.[5]

The equations for relating ν_N and ν_Y to experimental measurements are the same as those used previously[4,5] (the "three-constant Mooney–Rivlin model" equations[2]) with C_{1X} replaced by C_{1Y}. Thus, the ratio ν_Y/ν_N is obtained from λ_0 and λ_s as follows:

$$\nu_Y/\nu_N = \lambda_0^2(1 - \lambda_s^3)[\psi_N + (1 - \psi_N)\lambda_s]/(\lambda_s^3 - \lambda_0^3)\lambda_s \quad (5)$$

If the dual network is stretched to a stretch ratio λ ($>\lambda_s$), the contributions to the true equilibrium stress σ from the two individual networks are

$$\sigma_N = \nu_N RT[(1 - \psi_N)(\lambda^2 - 1/\lambda) + \psi_N(\lambda - 1/\lambda^2)] \quad (6)$$

$$\sigma_Y = \nu_Y RT[\lambda^2/\lambda_0^2 - \lambda_0/\lambda] \quad (7)$$

$$\sigma = \sigma_N + \sigma_Y \quad (8)$$

The additivity expressed in eq 8 can be tested experimentally as will be shown. If the equilibrium stress is measured at a stretch ratio λ_0' as close as possible to λ_0, the contribution σ_Y from eq 7 is very small and ν_N can be determined from eq 6 with a correction from eq 5 and 7 which is usually negligible. From this and eq 5, ν_Y is determined. If the degree of cross-linking is slight (low irradiation dose, low ν_X), the approach to equilibrium stress may be quite slow because of slow relaxation processes attributed to untrapped entanglements remaining on dangling branched structures[4] which are irrelevant to the present calculations but may necessitate holding the networks at λ_0' for long periods.

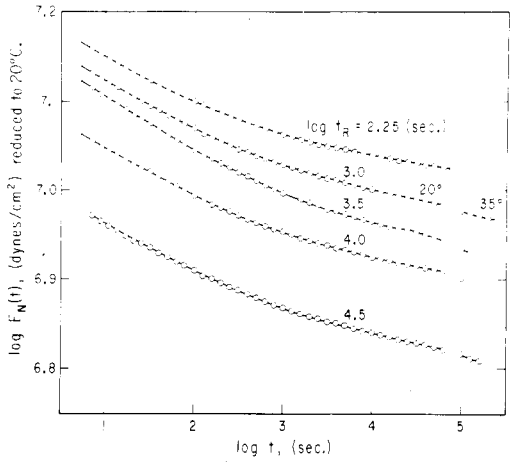

Figure 1. Time-dependent Young's modulus $E_N(t)$ calculated from stress relaxation measurements at $\lambda_0' \simeq \lambda_0 \simeq 1.6$, plotted logarithmically against time, for various initial relaxation periods t_R as indicated followed by irradiation with 3.0×10^{20} eV/g. Temperature during stress relaxation measurements initially 20 °C followed by an increase to 35 °C.

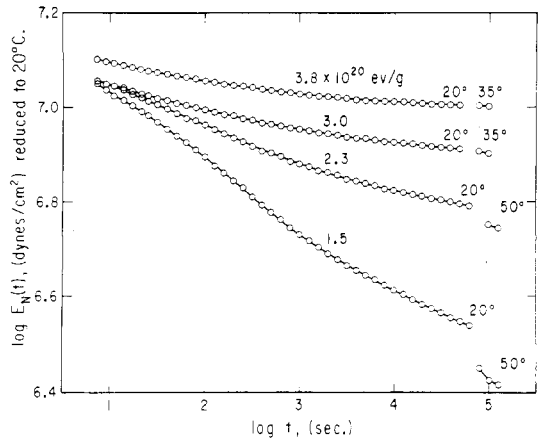

Figure 2. Time-dependent Young's modulus $E_N(t)$ as in Figure 1 for a relaxation period $t_R = 10^4$ s followed by irradiation with different doses as indicated. Temperatures of stress relaxation measurements are indicated.

There is one small inconsistency in the use of eq 6–8 for stretch ratios $\lambda > \lambda_0$; here, the Y network as well as the N network is in extension rather than compression, and the NR contribution to the stress (but not the X contribution[9]) should probably have a C_2 component. However, in practice measurements are not made with λ much greater than λ_0 because the samples break.

Experimental Section

The 1,2-polybutadiene used in these experiments was that identified as polymer C in previous publications,[4,5] containing 96% 1,2-(vinyl) microstructure, number- and weight-average molecular weights 0.96×10^5 and 1.61×10^5, respectively, and T_g estimated as −10 °C. It was generously supplied by Dr. G. G. A. Böhm of the Firestone Tire and Rubber Co.

The procedures for preparing, stretching, and irradiating samples with a ^{60}Co source have been described.[4,5] The strips, cut from films cast from 5% benzene solution, were 6-cm long, 0.6-cm wide, and 0.07-cm thick. The stretching to λ_0 was done at 0 °C within 30 s or slightly less, and subsequent relaxation occurred at constant λ_0 at 0 °C for periods t_R from 3 min to 8.8 h; the strip was attached to a steel band on which it remained mounted during irradiation so λ_0 (usually about 1.6) could be measured accurately afterward. (The stress decay could not be measured but could be estimated from previous experiments under the same conditions,[5] so that the total density of effective entanglement strands $\nu_e(t)$ could be calculated. It is obtained as $\nu_e(t) = (2/RT)[C_1(t) + C_2(t)]$, where the C's are derived from Mooney–Rivlin analysis of the stress relaxation of the uncross-linked polymer.[5,10,11]) Following t_R, the strip was quickly cooled to −15 °C, transported to the ^{60}Co source, and irradiated at −10 °C under vacuum.

The stretch ratios λ_0 and λ_s (after equilibrium retraction to the state of ease) were measured with a travelling microscope focussed on fiducial marks. Subsequently, stresses at $\lambda_0' \simeq \lambda_0$ were measured as a function of time, first at 20 °C and later at a higher temperature to hasten the approach to equilibrium to determine ν_N from eq 6. The value of ψ_N corresponding to the given t_R was obtained from the stress relaxation measurements on the uncross-linked polymer mentioned above.[5,11] Then, in some cases, stress–strain measurements were made at various λ, allowing at least 30 min at 50 °C to approach equilibrium to test eq 8. The apparatus for stress measurement and recording has been described elsewhere.[12]

The experimental procedure is summarized in Table I.

Results

The approach to equilibrium stress at $\lambda_0' \simeq \lambda_0$ is illustrated in Figures 1 and 2, first for a series of samples with the same irradiation dose but different initial relaxation periods t_R prior to irradiation (Figure 1) and then for a series with the same t_R but different doses (Figure 2). Here the time-dependent Young's modulus $E_N(t)$ is plotted logarithmically against time; it is defined[4] as

$$E_N(t) = 3\sigma(t)/[(1 - \psi_N)(\lambda_0'^2 - 1/\lambda_0') + \psi_N(\lambda_0' - 1/\lambda_0'^2) + (\nu_Y/\nu_N)(\lambda_0'^2/\lambda_0^2 - \lambda_0/\lambda_0')] \quad (9)$$

so that, in accordance with eq 6–8, $E_N(\infty) = 3\nu_N RT$. Equilibrium is not quite reached, but in view of the large ordinate scale it is believed that the final measurements at an elevated temperature are close to the equilibrium values. It is evident that ν_N decreases with increasing t_R (because more of the entanglements relax before being trapped) and increases with increasing dose (because higher cross-linking gives a larger number of cross-link points per original molecule and hence a higher trapping probability.[6])

For samples cross-linked with a constant dose of 3.0×10^{20} eV/g, Figure 3 shows the following strand densities plotted against log t_R: $\nu_e(t)$, terminated by total unrelaxed entanglements; ν_N, terminated by trapped unrelaxed entanglements; and $\nu_Y = \nu_X + \nu_{NR}$, terminated by cross-links or trapped relaxed entanglements. Both $\nu_e(t)$ and ν_N decrease, of course, with increasing t_R. The sum ν_Y is at first constant with a value of 0.70×10^{-4} mol/cm^3 which may be identified with ν_X since there will be a lag before establishment of trapped relaxed entanglements (see Discussion below). The difference $\nu_Y - 0.70 \times 10^{-4}$ may be identified with ν_{NR}, trapped relaxed entanglements, shown by the dashed curve.

A similar decrease in ν_N and increase in ν_Y for a single relaxation period t_R has been reported by Hvidt and Kramer.[13]

When the irradiation dose is varied, both ν_N and ν_Y increase with dose, as shown in Figure 4. Of course, ν_X increases with the extent of the cross-linking reaction, while both ν_N and ν_{NR} increase because of enhanced trapping probability. For all doses, ν_N decreases and ν_Y increases with increasing t_R, as observed for a specific dose in Figure 3. The data are a little scattered because the extent of cross-linking reaction at a given dose is subject to some random error associated with the geometry of the irradiation mounting. The ratio ν_Y/ν_N increased progressively with cross-linking.

The data presented in these figures refer to samples cross-linked at $\lambda_0 \simeq 1.6$. In other experiments, λ_0 was varied from about 1.35 to 2.0 for a dose of 3.0×10^{20} eV/g, and it was found that ν_N, ν_X, and ν_{NR} were essentially

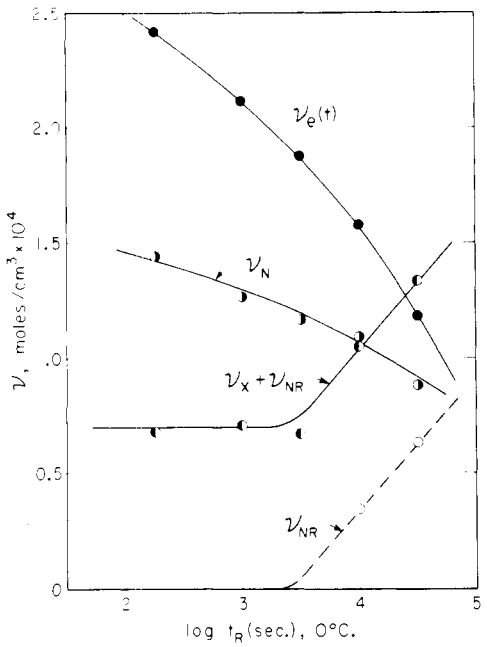

Figure 3. Concentrations of unrelaxed entanglement strands $\nu_e(t)$, trapped unrelaxed entanglement strands ν_N, and cross-link strands plus trapped relaxed entanglement strands $\nu_Y = \nu_X + \nu_{NR}$, calculated from eq 5 and 9, plotted against log t_R in seconds. (Dose 3.0×10^{20} eV/g, $\lambda_0 \simeq 1.6$.)

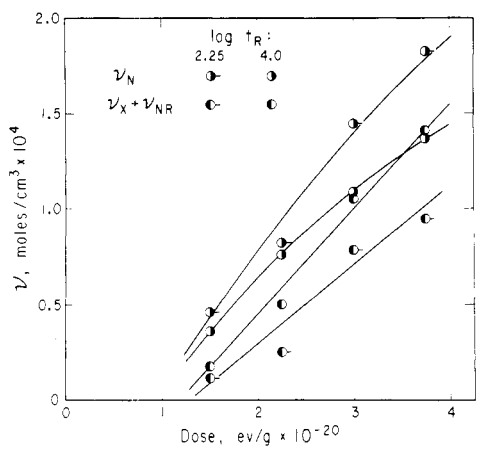

Figure 4. Increases in ν_N and $\nu_Y = \nu_X + \nu_{NR}$ with irradiation dose, corresponding to two different initial relaxation periods log t_R(s) = 2.25 and 4.0, respectively ($\lambda_0 \simeq 1.6$).

independent of λ_0. This result, which will be described elsewhere,[11] confirms the utility of the three-constant Mooney–Rivlin formulation upon which all these calculations are based.

We turn now to tests of the additivity of the stresses of the two individual networks of the dual network model (eq 8). This has been accurately confirmed for the case where there is no initial relaxation and $\nu_{NR} = 0$, for both stress and birefringence.[5] In the present experiments, it can be tested by calculating σ_N and σ_Y obtained from λ_0, λ_s, and σ at $\lambda_0' \simeq \lambda_0$ and comparing their sum with experimental values of σ. This is represented in Figures 5 and 6 for a cross-linking dose of 3.0×10^{20} eV/g and two different initial relaxation periods, log t_R (in seconds) = 3.5 and 4.5. The agreement is excellent, showing that the additivity holds when trapped relaxed entanglements are included. All numerical data will be recorded elsewhere.[11]

Discussion

From the data of Figure 3, the trapping probabilities of relaxed and unrelaxed entanglements can be estimated

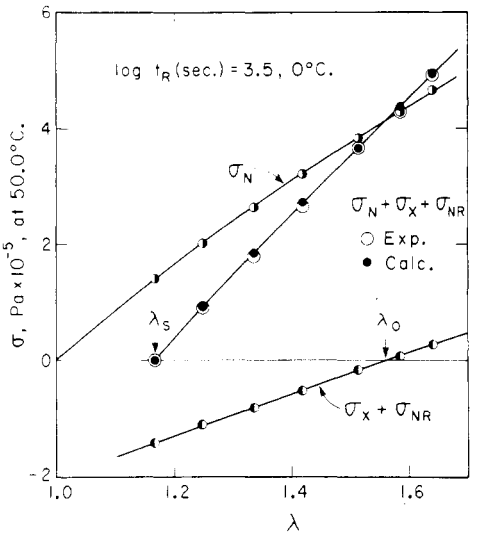

Figure 5. Stress–strain curves calculated for N network, Y network, and their sum; also experimentally measured, for log t_R(s) = 3.5, dose 3.0×10^{20} eV/g ($\lambda_0 = 1.560$, $\lambda_s = 1.166$, $\nu_N = 1.164 \times 10^{-4}$ mol/cm^3, $\nu_Y = 0.673 \times 10^{-4}$ mol/cm^3, $\psi_N = 0.725$).

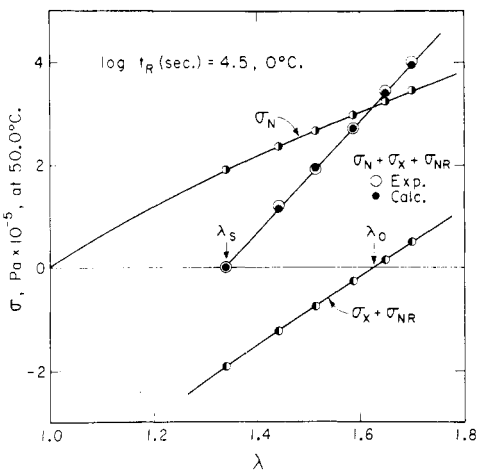

Figure 6. Stress–strain curves calculated for N network, Y network, and their sum; also experimentally measured, for log t_R(s) = 4.5, dose 3.0×10^{20} eV/g ($\lambda_0 = 1.626$, $\lambda_s = 1.339$, $\nu_N = 0.882 \times 10^{-4}$ mol/cm^3, $\nu_Y = 1.335 \times 10^{-4}$ mol/cm^3, $\psi_N = 0.885$).

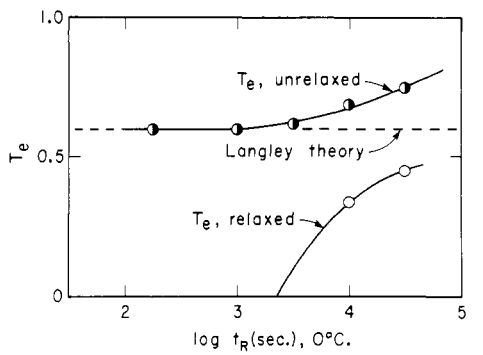

Figure 7. Entanglement trapping probabilities $T_{e,u}$ for unrelaxed and $T_{e,r}$ for relaxed entanglements calculated from measurements and compared with Langley theory.

separately by eq 1 and 2. For $T_{e,u}$, no further assumption is necessary. For $T_{e,r}$, an arbitrary estimate of ν_e^0 must be made; we take it as 2.6×10^{-4} mol/cm^3, being slightly higher than the maximum value of $\nu_e(t)$ observed and near the value estimated from viscoelastic properties for a similar polymer.[14] The results are shown in Figure 7 plotted against log t_R and compared with the prediction of the Langley theory. The latter is obtained as described

in paper 5 of this series;[4] from $\nu_X = 0.70 \times 10^{-4}$ mol/cm^3, the average number of cross-linked points per initial molecule (γ) is estimated to be 8.6, and T_e is found from Langley's graph (interpolated for $\bar{M}_w/\bar{M}_n = 1.7$) to be 0.62.

When the initial relaxation is slight, $T_{e,u}$ is independent of t_R and agrees with the Langley theory, as found previously.[4] After longer relaxation periods, the trapping probability of the unrelaxed entanglements increases. The trapping probability of the relaxed entanglements, $T_{e,r}$, is zero up to the point where $T_{e,u}$ begins to increase and then increases but remains smaller than the Langley prediction.

This behavior can be understood qualitatively in terms of the alternative tube model for the topological restraints of an entangled molecule as treated in detail recently by Doi and Edwards.[7,15,16] The final stage of relaxation in an uncross-linked polymer involves the escape of a molecule from its tube by diffusing back and forth along its contour.[17] In a state of strain, the ends regain a random configurational distribution finding new tube paths, progressing from the ends inward, while a steadily shrinking central portion remains confined in the deformed tube. The relaxed and unrelaxed entanglements can be identified with constraints on the ends and center, respectively. Whereas the Langley theory provides an average trapping probability, it is evident that the probability will be greater near the center of a molecule than near the ends. In fact, there is essentially no chance of trapping a relaxed entanglement until the randomized ends become longer than the average entanglement spacing and also longer than the average spacing between cross-linked points.

The average number of cross-linked points on a randomized end can be estimated as $(\gamma/2)(1 - \nu_e(t)/\nu_e^0)$. For the experiments of Figures 3 and 7, this becomes greater than 1 only for $\log t_R$ (s) $\simeq 3.5$, in agreement with the first appearance of trapped relaxed entanglements. This description ignores the possibility that some constraints even near the center of the molecule can be relieved by escape of other molecules from *their* tubes, but no attempt is made to take their complication into account at the present time.

Acknowledgment. This work was supported in part by the National Science Foundation, Grant No. DMR 76-09196, Polymers Program. We are indebted to Professor J. E. Willard for the use of the ^{60}Co source for irradiation, to Dr. G. G. A. Böhm for the polymer, to Dr. N. R. Langley, Dr. O. Kramer, and Mr. S. Hvidt for comments, and to Mr. D. Deubler for help with calculations.

References and Notes

(1) O. Kramer, R. L. Carpenter, V. Ty, and J. D. Ferry, *Macromolecules*, **7**, 79 (1974).
(2) R. L. Carpenter, O. Kramer, and J. D. Ferry, *Macromolecules*, **10**, 117 (1977).
(3) R. L. Carpenter, O. Kramer, and J. D. Ferry, *J. Appl. Polym. Sci.*, **22**, 335 (1978).
(4) R. L. Carpenter, H.-C. Kan, and J. D. Ferry, *Polym. Eng. Sci.*, in press.
(5) H.-C. Kan, R. L. Carpenter, and J. D. Ferry, *J. Polym. Sci., Polym. Phys. Ed.*, in press.
(6) N. R. Langley, *Macromolecules*, 1, 348 (1968).
(7) M. Doi and S. F. Edwards, *J. Chem. Soc., Faraday Trans. 2*, **74**, 1802 (1978).
(8) C. R. Taylor and J. D. Ferry, *J. Rheol.*, in press.
(9) J. D. Ferry and H.-C. Kan, *Rubber Chem. Technol.*, **51**, 731 (1978).
(10) J. W. M. Noordermeer and J. D. Ferry, *J. Polym. Sci., Polym. Phys. Ed.*, **14**, 509 (1976).
(11) H.-C. Kan, Ph.D. Thesis, University of Wisconsin, 1979.
(12) O. Kramer, R. Greco, J. D. Ferry, and E. T. McDonel, *J. Polym. Sci., Polym. Phys. Ed.*, **13**, 1675 (1975).
(13) S. Hvidt and O. Kramer, private communication; S. Hvidt, Cand. Scient. Thesis, University of Copenhagen, Denmark, 1978.
(14) J. D. Ferry, "Viscoelastic Properties of Polymers", 2nd ed., Wiley, New York, 1970, p 406.
(15) M. Doi and S. F. Edwards, *J. Chem. Soc., Faraday Trans. 2*, **74**, 1818 (1978).
(16) M. Doi, personal communication.
(17) P. G. de Gennes, *J. Chem. Phys.*, **55**, 572 (1971).

The pH of Weak Polyacid Solutions in the Presence of Mono- and Divalent Counterions

Masaaki Ishikawa

Department of Polymer Chemistry, Kyoto University, Kyoto, Japan.
Received October 4, 1978

ABSTRACT: The pH of weak polyacid solutions containing mono- and/or divalent counterions has been treated by use of the solution of the Poisson–Boltzmann equation applied to the parallel-rod cell model. The dielectric saturation effect is taken into account in the calculation. Agreement between the theory and experimental data is generally satisfactory, particularly if the comparison is carried out at a constant charge density. If the charge density of the polyelectrolyte is low and the ionic strength is high, however, the agreement between the theory and experiments is not satisfactory, probably because the parallel-rod cell model fails.

The pH of weak polyacid solutions is related to the surface electric potential of the polymer skeleton.[1] The surface electric potential can be numerically and analytically calculated from the Poisson–Boltzmann (PB) equation if we assume a parallel-rod cell model for the polyion.[2-8] Some investigators[6-8,10-13] have discussed the potentiometric titration curves of weak polyacids in the presence of 1–1 salts using the surface potential of the polymer thus calculated. However, there have been few studies in the presence of divalent counterions. In this work, we used quaternized ethylenediamine as the divalent counterion and compared the experimental potentiometric titration results with the surface electric potential calculated from the PB equation. Ordinary divalent cations such as Ca^{2+} and Ba^{2+} show site binding to polyacrylic acid (PAA) causing precipitation. Such precipitation is not observed in the titration with quaternized ethylenediamine.

Based on the counterion condensation concept of Manning, Manning and Holtzer[14] derived a theory of

0024-9297/79/2212-0498$01.00/0